



Synthesis, cytotoxic activity and binding model analysis of novel isoxazole-docetaxel analogues with C3'-N modification

Ming Chen¹ · Jiyuan Liu^{2,3} · Zhen Tian³ · Xueying Liu² · Shengyong Zhang²

Received: 16 October 2017 / Accepted: 1 February 2018
© Springer Science+Business Media, LLC, part of Springer Nature 2018

Abstract

Structure–activity relationship (SAR) studies confirm that modifications at C-3' position can lead to the development of highly potent novel taxoids. We designed and synthesized a series of novel isoxazole-docetaxel analogues **A1–A5** by introducing isoxazolyl groups to C3'-N position. All of the synthesized compounds exhibited similar to better cytotoxic activities than docetaxel against human cancer cell lines, Hela, A2780, A549, MCF-7, and SK-OV-3. These compounds also possessed higher inhibition than docetaxel against drug-resistant cancer cell lines, A2780-MDR and MCF-7-MDR. Binding model analysis of **A1–A5** molecule to microtubule (MT) showed that these compounds were anchored to the active site, explaining their inhibitory effects on MT in vitro. The calculated binding free energy values were in positive correlation with the IC₅₀ values of **A1–A5** compounds against cancer cells. These results strongly support the statement that the introduction of isoxazolyl groups to C-3' position indeed improves the cytotoxic activities of taxoids.

Keywords Docetaxel · Isoxazole · Cytotoxic · Inhibition · Binding model analysis

Introduction

Cancer has been one of the most deadly diseases in the world characterized by uncontrolled cell divisions. Chemotherapy is one of the most common cancer treatments. Among a variety of chemotherapeutic drugs, taxoids paclitaxel, and docetaxel (Fig. 1), which act as promoters of tubulin assembly, as well as inhibitors of the disassembly process, are two of the most important drugs currently in the

fight against various cancers, such as metastatic breast cancer, advanced ovarian cancer, non-small cell lung cancer, and Kaposi's sarcoma (Rowinsky 1997; Mekhail and Markman 2002). However, the treatment with these taxoids caused intractable obstacles such as multidrug resistance (MDR). Therefore, it is essential to develop novel taxoid anticancer drugs with fewer side effects, superior pharmacological properties, and improved activity against various classes of cancers, especially drug-resistant cancers. Related studies on structure–activity relationship (SAR) of taxoids have indicated that the C3' amide-acyl group at the side-chain is an extremely crucial site for the bioactivity (Kirikae et al. 1996, 1998; Fu et al. 2009), but many different *N*-acyl groups may be tolerated and some groups have improved activity. Currently, numerous analogues with C3'-*N* modification have been designed and prepared to develop novel taxoids (Georg et al. 1992a, b, 1994; Gunda et al. 1992; Roh et al. 1999, 2002; Ojima et al. 2003; Lu et al. 2011; Chang et al. 2013). Roh et al. had synthesized a series of C3'-*N*-acyl-*N*-debenzoyl paclitaxel analogues, some of which exhibited higher cytotoxicities (up to 20-fold) and stronger abilities to induce apoptosis than paclitaxel (Roh et al. 1999, 2002). In 2003, through the replacement of the C3'-*N*-benzoyl group with the different aromatic rings, Ojima et al. pointed out that paclitaxel analogues bearing a 4-methylbenzoyl and a 4-chlorobenzoyl group showed higher activities than paclitaxel (Ojima et al. 2003).

These authors contributed equally: Ming Chen and Jiyuan Liu.

Electronic supplementary material The online version of this article (<https://doi.org/10.1007/s00044-018-2151-7>) contains supplementary material, which is available to authorized users.

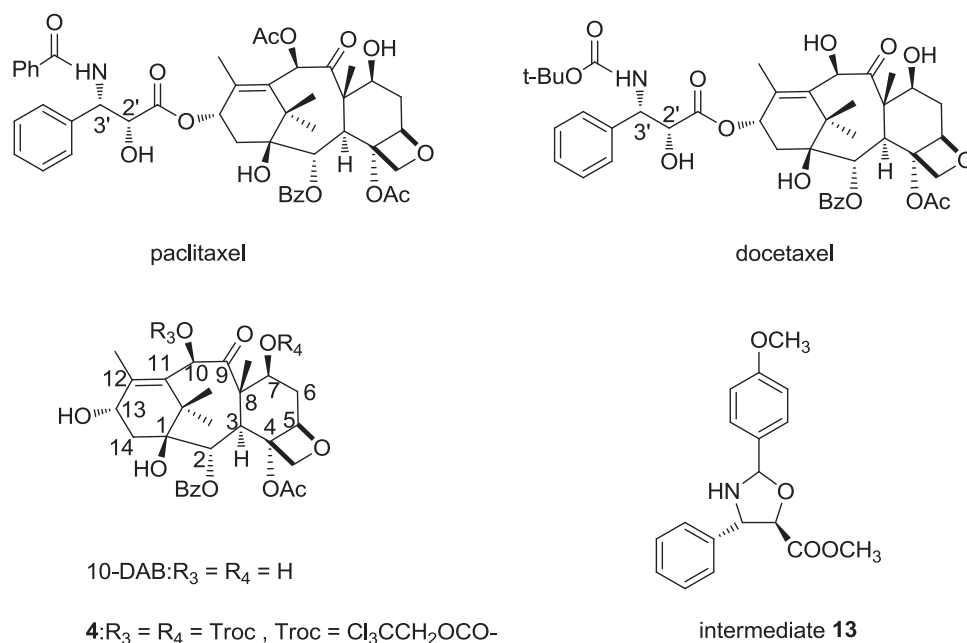
- ✉ Xueying Liu
xyliu0427@163.com
- ✉ Shengyong Zhang
syzhang@fmmu.edu.cn

¹ Department of Pharmacy, The 309th hospital of PLA, 17 Heishanhu Road, Haidian District, Beijing 100091, China

² Department of Medicinal Chemistry, School of Pharmacy, Fourth Military Medical University, Xi'an 710032 Shanxi, China

³ Key Laboratory of Plant Protection Resources & Pest Management of the Ministry of Education, College of Plant Protection, Northwest A&F University, Yangling, Shanxi 712100, China

Fig. 1 The structure of paclitaxel, docetaxel, and intermediate **13**



Just recently, Chang et al. synthesized a series of novel C3'-N-alkoxycarbonyl docetaxel analogues, some of which were fluorinated. These compounds exhibited similar potency to docetaxel and greater potency than paclitaxel against the SK-OV-3 and A549 cell lines (Chang et al. 2013). Meanwhile, Kingston et al. also concluded that design and synthesis of a highly cytotoxic tubulin-assembly agent should be based on the effective binding site of the taxane (Kingston and Snyder 2014). In general, these reported results encourage us to make further efforts to investigate the critical site.

In recent years, isoxazole scaffold has attracted more and more attention because of its potent bioactivity. A number of novel compounds containing isoxazole scaffold were prepared and evaluated as different inhibitors depending on protein-ligand binding (Ji et al. 2008; Lilienkamp et al. 2009; Baruchello et al. 2011; Rowbottom et al. 2012). Michaelides et al. developed a series of benzoisoxazoles analogues and evaluated their bioactivity as inhibitors of receptor tyrosine kinases (RTKs) (Ji et al. 2008). SAR studies confirmed these analogues had potent inhibitory effects on both the vascular endothelial growth factor receptor (VEGFR) and platelet-derived growth factor receptor families of RTKs. Recently, Baruchello et al. launched some novel 3,4-isoxazolidiamides as potent inhibitors of chaperone heat shock protein 90 through a structural investigation on the isoxazole scaffold (Baruchello et al. 2011).

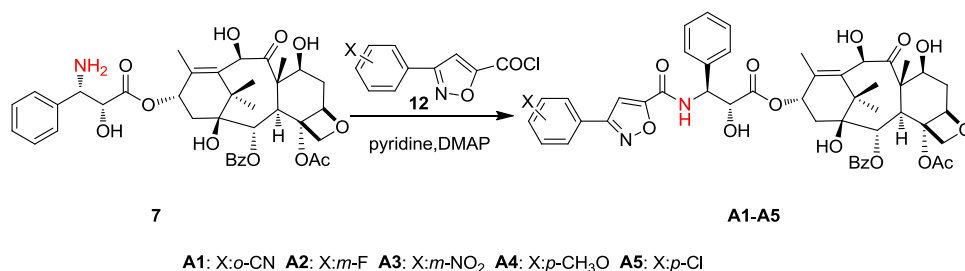
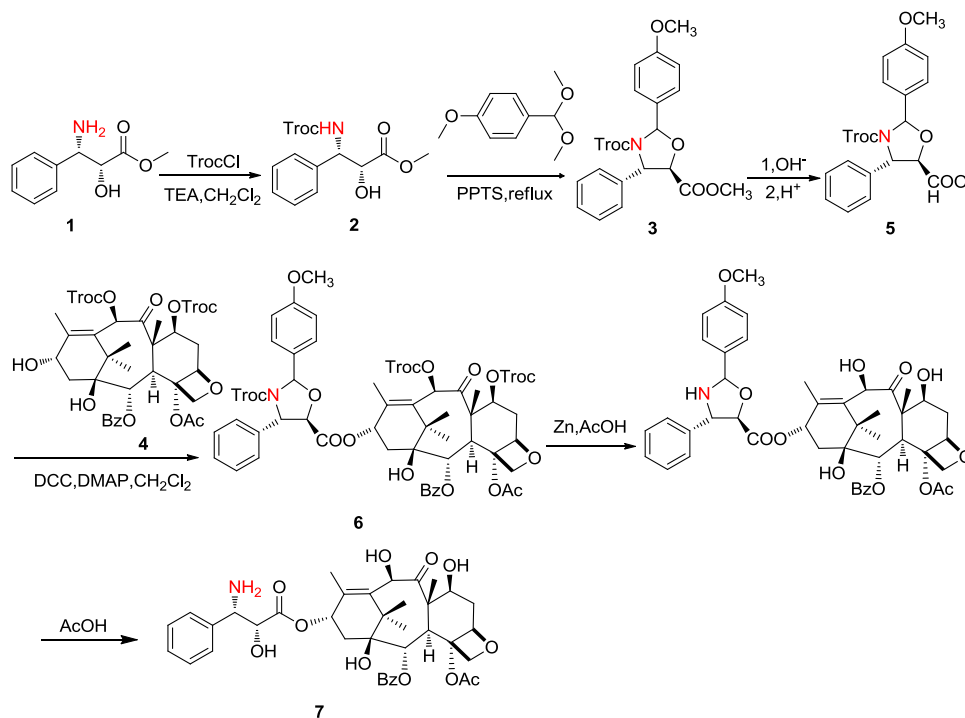
Based on available information, we hypothesized that the introduction of isoxazolyl group to the C3'-N site of

docetaxel would improve its affinity to the target protein, further enhancing the cytotoxic activity. Therefore, in the present study, novel isoxazole-docetaxel analogues were designed and synthesized by introducing 3-aryl-isoxazole-5-carbonyl groups to the C3'-N-amino-docetaxel, and their cytotoxic activities on different cancer cell lines were evaluated. Molecular simulations including molecular docking and binding free energy calculations were performed as well to reveal the binding modes between the synthesized compounds and microtubule (MT). Our study probes the optimization of novel taxoids with higher cytotoxic activity.

Results and discussion

Synthesis

Under the conditions of classic amide formation, five isoxazole-docetaxel analogues (**A1–A5**) were prepared through the acylation of C3'-amino-docetaxel with 3-aryl-isoxazole-5-carboxylic acids. Thus, the reactions of the key intermediate **7** with 3-aryl-isoxazole-5-carboxylic acid chloride **12** in pyridine using 4-dimethylamopyridine (DMAP) as catalyst at room temperature gave C3'-N-(3-aryl-isoxazole-5-acyl)docetaxel (**A1–A5**) in good yields (Scheme 1). It is noteworthy that the replacement of conventional triethylamine–dichloromethane reaction system with current pyridine condition could ensure selective acylation of amino prior to other active groups (Swindell and Krauss 2001).

Scheme 1 General synthetic route for compounds **A1–A5****Scheme 2** The synthetic route of **7**

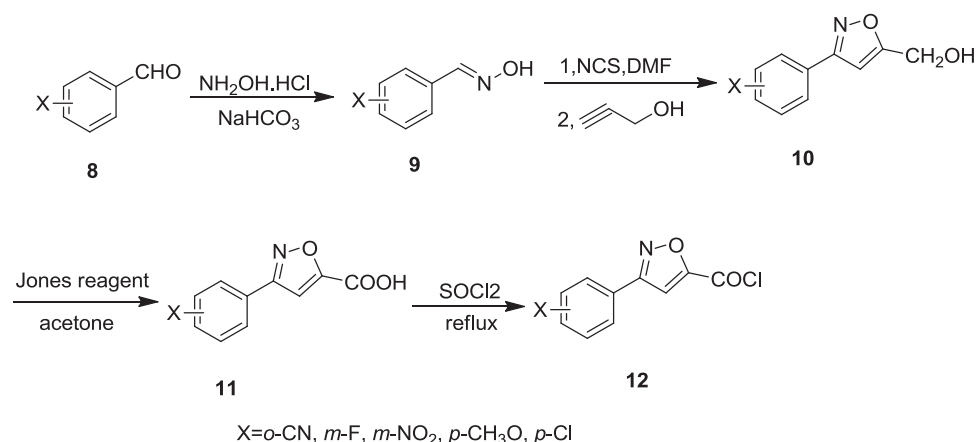
The synthesis of **7** started from (2*R*,3*S*)-3-phenylisoserine methyl ester **1** in five steps. We found that the compound **13** (Fig. 1) which is an intermediate in an alternative synthetic route to compound **7**, is unstable and prone to remove the protecting group in acidic condition if H atom at N site is exposed. Based on this, we designed the synthetic route of **7** outlined in Scheme 2, the advantage being that *p*-methoxybenzaldehyde was removed automatically accompanied with de-protection of Troc. Compounds **2**, **3**, and **5** were prepared according to the literature (Hayashi et al. 2003). Then, the coupling of carboxylic acid **5** with 7,10-di-Troc-10-deacetylbaccatin **4** (Fig. 1) in the presence of dicyclohexylcarbodiimide (DCC) and DMAP furnished the corresponding esters **6** with a high yield (94.8%). Finally, the de-protection of all of the protective groups simultaneously at C-7, C-10, and C-13 side chain sites of **6** with zinc powder in AcOH/AcOEt system at room temperature gave the key intermediate **7**, a white powder, with a good yield after purification (91.2%). Our design ensured a higher

yield and purity of compound **7** comparing with Commerçon's (Didier et al. 1994).

The synthesis of 3-aryl-isoxazole-5-carboxylic acid chloride **12** were carried out using the inexpensive substituted benzaldehydes **8** as the starting materials in four steps according to the literatures (Scheme 3) (Shang and Wang 2002). The reactions of acids **11** with thionyl chloride allowed for the corresponding acyl chloride **12**.

Cytotoxicity

The cytotoxicities of these novel analogues (**A1–A5**) were evaluated against five normal human cancer cell lines (HeLa, A2780, A549, MCF-7, and SK-OV-3), and two drug-resistant tumor cell lines (A2780-MDR and MCF-7-MDR) by standard MTT assay (Mosmann 1983; Lamberth et al. 2007), docetaxel was used as positive control. As shown in Table 1, all five novel analogues exhibited similar to better inhibitory activities against the five cancer cell

Scheme 3 The synthetic route of **12****Table 1** The cytotoxic activities of analogues (**A1–A5**) against human cancer cell lines

Analogues	Cancer cell cytotoxicity IC ₅₀ (nM) ^a						
	Hela	A2780	A2780-MDR ^b	A549	MCF-7	MCF-7-MDR ^c	SK-OV-3
A1	35.4	9.0	40.8	32.7	38.2	191.0	37.2
A2	25.1	12.3	60.5	23.2	16.6	116.8	26.9
A3	38.8	13.4	66.5	35.6	39.0	112.1	28.8
A4	75.8	13.7	65.6	30.7	57.8	115.2	20.3
A5	24.0	8.9	46.4	39.5	20.0	143.8	15.1
Docetaxel	50.1	33.1	126	35.2	38.5	180	37.1

^aIC₅₀: concentration which produces 50% inhibition of proliferation after 72 h of incubation. HeLa: cervical cancer, A2780: ovarian cancer, A549: non-small cell lung cancer, MCF-7: breast cancer, SK-OV-3: ovarian cancer

^bA2780-MDR: multidrug-resistant ovarian cancer

^cMCF-7-MDR: multidrug-resistant breast cancer

lines comparing with docetaxel. Among these five novel analogues, **A1** and **A5** were approximately four times stronger than docetaxel in the activity against A2780, **A5** possessed the highest potencies against Hela, A2780, and SK-OV-3. Meanwhile, **A2** exhibited the best activity against A549 and MCF-7. What's more, all of these compounds improved the sensitivity of those drug-resistant tumor cells, A2780-MDR and MCF-7-MDR. Especially, **A1** and **A5** exhibited about three times stronger activity against A2780-MDR.

Effects on cytoskeleton

To further investigate whether the tested drugs have effects on cytoskeleton, we employed immunofluorescence techniques. As shown in Fig. 2, when exposed to the five tested compounds, the cytoskeleton of Hela cell lines were obviously disrupted and displayed the disperse condition compared to the integrity of control, suggesting that these

compounds have negative effects on cytoskeleton in the present study.

Binding model analysis

By using molecular docking, the accurate binding mode of paclitaxel-tubulin was obtained (reference to supporting information Fig. S1). The conformations superimposition of paclitaxel from the crystal structure of paclitaxel-tubulin complex (PDB ID: 2HXF) (color: gray) and the docking one (color: cyan) revealed quite minute root-mean-square deviation (RMSD, 0.075 Å), indicating that the docking works of the compounds (**A1–A5**) were accurate in the binding site. As shown (Fig. 3), hydrogen bond nets were vital to the binding of compounds **A1–A5** to tubulin. The five compounds all formed hydrogen bonds with the backbone of Arg275. Specifically, for **A1**, **A4**, and **A5**, the hydrogen bond interaction was detected between the backbone OH (1 position) and the O atom on Arg275, whereas for **A2** and **A3**, the hydrogen bond occurred between the O from isoxazole group and the NH from Arg275. Besides, the hydroxyl (10 position) on the backbone of **A3** formed a hydrogen bond with NH group from the sidechain of Arg275 as well. Gly359 from tubulin was involved in the hydrogen bond interaction, the O from its sidechain formed a hydrogen bond with the backbone OH (7 position) of **A1**, **A2**, **A4** and **A5**, respectively. For compounds **A3** and **A4**, it is noteworthy that two extra hydrogen bonds were detected in their interactions with tubulin. By introducing nitro to the phenyl-isoxazole group in **A3**, the nitro could form hydrogen bonds with backbone NH and side chain O of Thr281, respectively. While in compound **A4**, the addition of methoxy to the phenyl-isoxazole group led to the formation of hydrogen bond between the oxygen bridge (5 position) of its backbone and the side chain NH of Arg281. Meanwhile, the hydrogen bond interaction also occurred between the backbone NH of Arg281 and the carbonyl (4 position) from the skeleton of **A4**. As a whole, the introduction of phenyl-

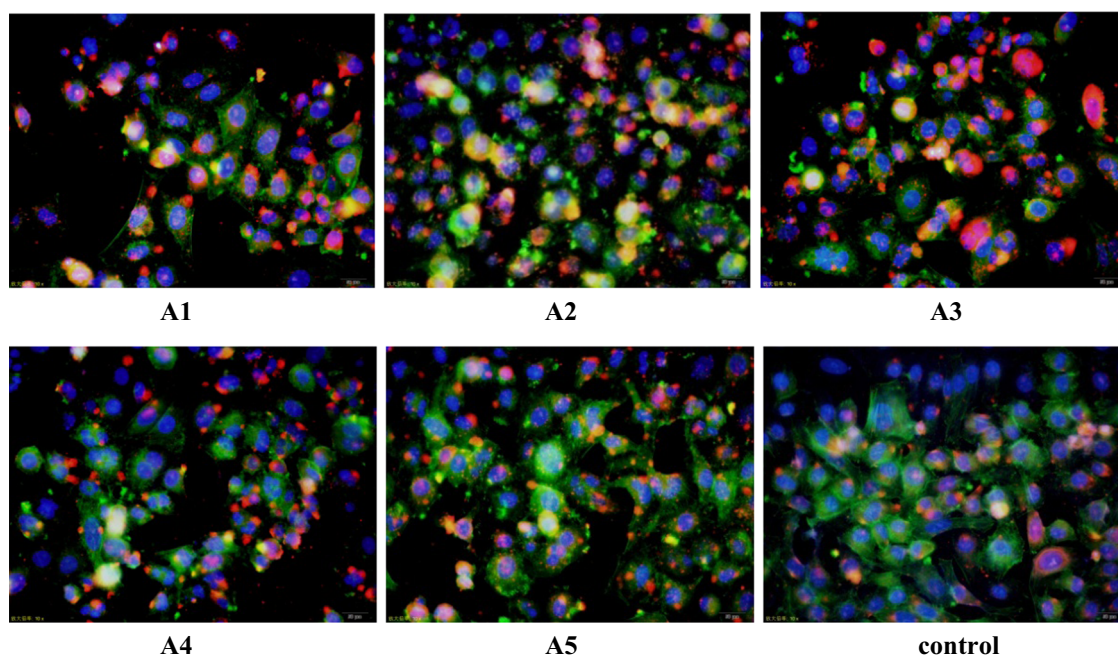


Fig. 2 Confocal images of HeLa cell lines left untreated (control), or exposed to the tested compounds (**A1–A5**) for 24 h. The compounds disrupted the microfilament-associated structure of F-actin (green) and Tubulin (red). Nuclear DNA was labelled in blue with Hoechst (color figure online)

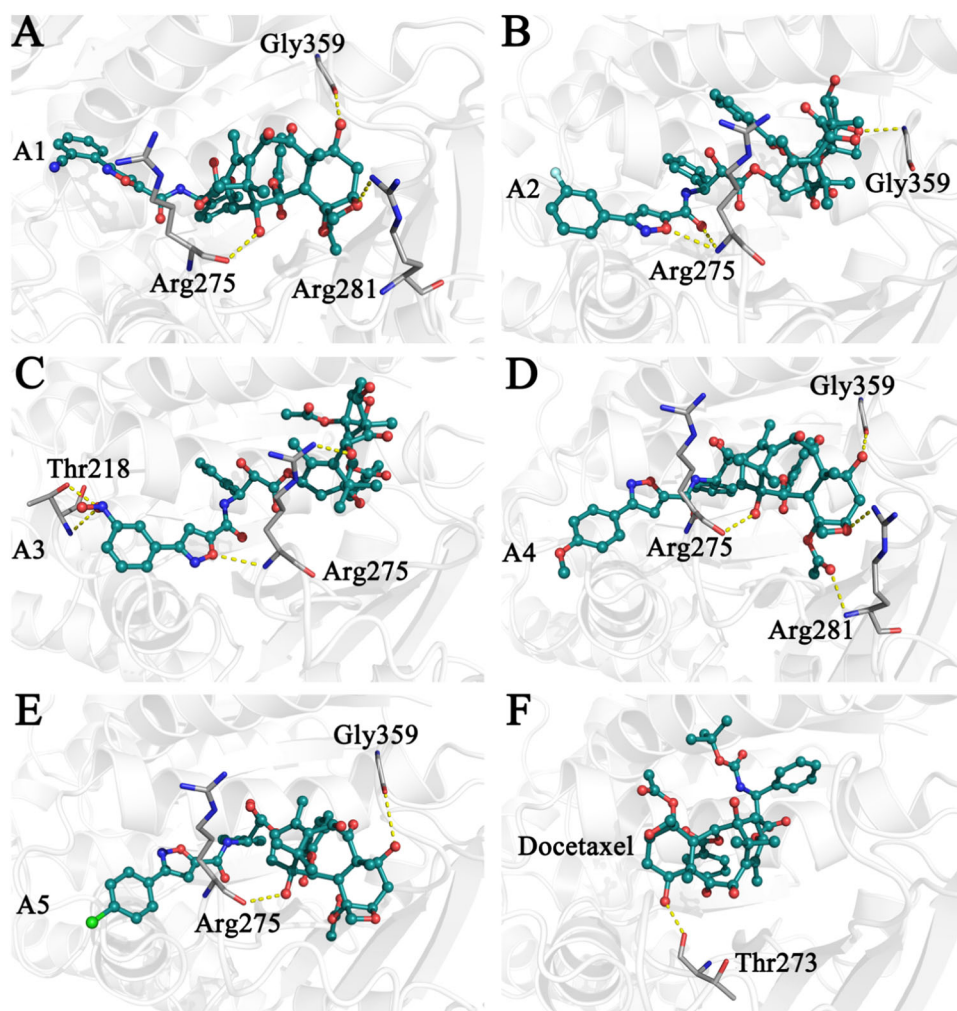
isoxazole group to the C3'-*N* position of docetaxel helps to form more hydrogen bonds in the active cavity of tubulin, this change may contribute to the higher cytotoxic activity of **A1–A5**. Not only that, the differences between the hydrogen bond nets of each complex are considered as a factor in affecting the activity of **A1–A5**.

Binding free energy

The binding free energy and the energy contribution components for compounds **A1–A5** and docetaxel were listed in Table 2. For the five tested compounds, **A1**, **A3**, **A4**, and **A5** caused higher binding free energy changes (ΔG) of tubulin than docetaxel, with **A2** being an exception. This fitted well with their corresponding cytotoxic activities, the one (**A5**) with the highest ΔG possessed the highest activity against cancer as well. By using docetaxel as control, the binding free energy items of **A1–A5** were analyzed and compared in detail. For **A2** which is characterized by the introduction of fluorine to the meta-position of phenyl-isoxazole group, the optimization shed negative effects on its lipophilic energy term [$S(\text{lipo})$] contributions, with $S(\text{lipo})$ less than the counterpart of docetaxel. As for **A3**, the introduction of nitro caused the significant increase of hydrogen bond energy [$S(\text{hbond})$] contribution but decrease of $S(\text{lipo})$, making its resultant ΔG only slightly higher than the counterpart caused by docetaxel. In the present study, introducing methoxy group (**A4**) and chlorine group (**A5**)

individually to the para-position of phenyl-isoxazole groups significantly raised the $S(\text{lipo})$ and $S(\text{hbond})$ values. Furthermore, the introduction of nitrile to the ortho-position of phenyl-isoxazole group in **A1** also shed positive effects on $S(\text{hbond})$ contributions. To reveal the reasons involved in the energy changes mentioned above, the superimposition of the binding modes of **A1–A5** was performed (Fig. S2). As shown, the binding modes of **A2**, **A4**, and **A5** were of high similarity, particularly for **A2** and **A5**, their conformations were close to perfect overlap. However, **A4** was characterized by the special H-bond nets. By introducing the phenyl-isoxazole group, a new H-bond was formed between the oxygen bridge from **A4** (5 position) and the main chain NH of Arg281 (4 position), hence higher $S(\text{hbond})$ was detected in **A4**. The differences between $S(\text{lipo})$ values of **A2** and **A5** can be attributed to the fact that the chlorine on para-position of phenyl (**A5**) contributed more to the $S(\text{lipo})$ than the fluorine on meta-position of phenyl (**A2**). Comparing with the chlorine group (**A5**), the greater exposure of methoxy group (**A4**) to the solvent contributed to the lower $S(\text{lipo})$ value. Similar phenomenon was also detected in **A3**, the introduction of nitro to the meta-position of phenyl-isoxazole group led to the exposure of 10-DAB (**A3**), causing the loss of $S(\text{lipo})$. Based on available data above, it is reasonable to speculate that introducing nitrile group and chlorine group to the ortho-position and para-position of phenyl-isoxazole group respectively has potential in increasing $S(\text{lipo})$ and S

Fig. 3 The carton representation of tubulin 3D model around the binding site of Docetaxel and its analogs (A1–A5). The binding model of tubulin with A1 (a), with A2 (b), with A3 (c), with A4 (d), with A5 (e), and with docetaxel (f). Docetaxel and its analogs (A1–A5) are presented as stick and sphere model. Cyan C; Red O; Blue N; Light blue F; Green Cl. Key residues are presented with the stick model. Color code: Gray C; Red O; Blue N. the yellow dotted lines show hydrogen bonds among the atoms from amino acid residues and docetaxel and its analogs (A1–A5) (color figure online)



(hbond) contributions simultaneously, further enhancing ΔG values of taxoids. However, future experiments are required to verify this speculation.

Conclusion

In summary, a series of novel C3'-N-(3-aryl-isoxazole-5-acyl)docetaxel analogues (A1–A5) were synthesized and characterized by ^1H nuclear magnetic resonance (NMR), ^{13}C NMR, and high resolution mass spectrometry (HRMS) analysis. The cytotoxicities were evaluated against various human cancer cell lines. The results showed that each of these five novel analogues possessed similar to better inhibitory activity than docetaxel. As revealed by binding mode and binding free energy analysis, the formation of more hydrogen bonds and differences in hydrogen bond nets were considered to be related to the cytotoxic activities of compounds A1–A5. The introduction of foreign groups (fluorine, nitro, nitrile, methoxy group and chlorine group) to the phenyl-isoxazole group did help in increasing the affinity of

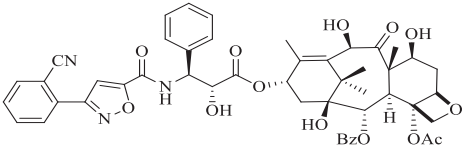
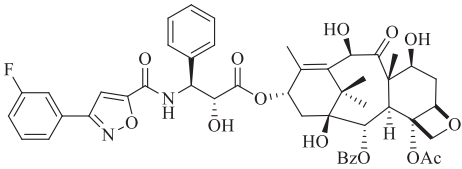
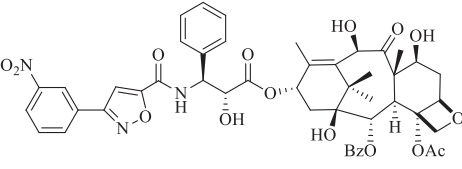
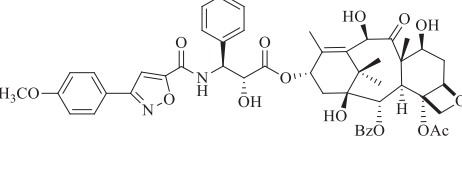
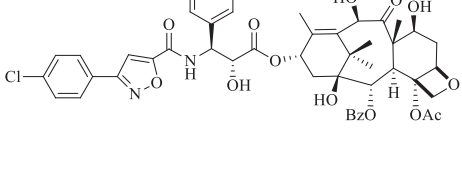
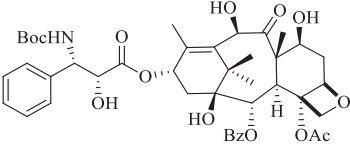
docetaxel analogues to tubulin, consequently improving cytotoxic activities of taxoids. These facts proved that the *t*-Boc group at the C3'-N position, which is the "gold standard," can be replaced by isoxazolyl groups without losing potency. Due to these findings, further SAR studies at C3'-N position of docetaxel are underway in our lab.

Experimental

General analytical procedures

Reagents and solvents were obtained commercially and used without further purification. Thin layer chromatography was carried out on Merck silica gel 60F plates. Flash column chromatography was performed on silica gel (200–300 meshes) from Qingdao Marine Chemical Factory in China. Melting points were determined on a Yanaco MP-500D melting point apparatus and were uncorrected. ^1H NMR and ^{13}C NMR spectra were recorded on a Bruker NMR AVC500 spectrometer in dimethyl sulfoxide

Table 2 The predicted binding free energy changes and the individual energy terms for the ligands

Analogues	Structure	S(hbond)	S(lipo)	H(rot)	ΔG (KJ/mol)
A1		2.13	318.29	5.58	-35.55
A2		1.11	239.73	5.50	-23.15
A3		3.19	230.82	5.66	-28.67
A4		2.30	323.46	5.62	-36.62
A5		1.89	354.13	5.39	-39.42
Docetaxel		0.37	269.76	5.67	-23.78

All values are given in KJ/mol

(DMSO)-d₆ or CDCl₃ using TMS as an internal standard. HRMS (FAB) analysis was carried out by the Central Lab of Nankai University.

General procedure for the synthesis of C3'-N-(3-aryl-isoxazole-5-acyl) docetaxel (A1–A5)

To a stirred solution of **7** (0.1 g, 0.14 mmol) and DMAP (2 mg, 0.014 mmol) in pyridine (3 mL) was added 3-aryl-

isoxazole-5-carboxylic acid chloride **12** (0.154 mmol) at room temperature. After 1 h, the mixture was diluted with methylene chloride, washed with 1N HCl, water, dried over MgSO₄ and concentrated to get a crude compound, which was purified by column chromatography (CH₂Cl₂:MeOH = 10:1) to furnish the corresponding C3'-N-(3-aryl-isoxazole-5-acyl)docetaxel (**A1–A5**) as a white solid.

C3'-N-[3-(2-cyanophenyl) isoxazole-5-acyl]docetaxel (A1)

Yield: 74.2%. m.p. 202–203.1 °C. ¹H NMR (500 MHz, CDCl₃) δ 8.16 (d, *J* = 7.2 Hz, 2H), 7.89–7.79 (m, 3H), 7.71 (td, *J* = 7.8, 1.2 Hz, 1H), 7.67–7.59 (m, 2H), 7.57–7.51 (m, 4H), 7.45 (t, *J* = 7.6 Hz, 2H), 7.39 (d, *J* = 7.3 Hz, 1H), 7.36 (s, 1H), 6.31 (t, *J* = 8.5 Hz, 1H), 5.83 (dd, *J* = 9.2, 2.5 Hz, 1H), 5.70 (d, *J* = 7.1 Hz, 1H), 5.25 (s, 1H), 4.97 (d, *J* = 9.4 Hz, 1H), 4.83 (d, *J* = 2.7 Hz, 1H), 4.33 (d, *J* = 8.5 Hz, 1H), 4.29–4.22 (m, 2H), 3.93 (d, *J* = 7.0 Hz, 1H), 3.50 (s, 2H), 2.64–2.53 (m, 1H), 2.42 (s, 3H), 2.37–2.29 (m, 2H), 2.27–2.22 (m, 1H), 2.09 (br, s, 1H), 1.91 (d, *J* = 13.9 Hz, 1H), 1.85 (s, 3H), 1.79 (s, 3H), 1.23 (s, 3H), 1.14 (s, 3H). ¹³C NMR (125 MHz, CDCl₃) δ 211.15, 171.94, 170.70, 166.85, 163.68, 161.05, 155.07, 137.91, 137.25, 136.29, 134.32, 133.81, 133.39, 130.91, 130.65, 130.21, 129.55, 129.32, 129.05, 128.72, 128.56, 127.11, 117.45, 110.97, 107.24, 84.26, 81.32, 78.66, 74.82, 74.53, 73.45, 72.30, 71.81, 57.72, 54.84, 50.82, 46.53, 43.05, 36.91, 35.91, 26.58, 22.61, 20.57, 14.47, 9.94. HRMS (FAB): calcd for C₄₉H₄₉N₃O₁₄ (M + Na⁺): 926.3107, found: 926.3103.

C3'-N-[3-(3-fluorophenyl) isoxazole-5-acyl]docetaxel (A2)

Yield: 72.1%. m.p. 193.5–195 °C. ¹H NMR (500 MHz, CDCl₃) δ 8.23 (d, *J* = 7.3 Hz, 2H), 7.86 (d, *J* = 9.3 Hz, 1H), 7.67 (t, *J* = 7.4 Hz, 1H), 7.57 (t, *J* = 7.7 Hz, 2H), 7.49 (d, *J* = 7.4 Hz, 2H), 7.45 (t, *J* = 7.5 Hz, 2H), 7.40 (d, *J* = 7.2 Hz, 1H), 7.38–7.35 (m, 1H), 7.34–7.31 (m, 1H), 7.21 (d, *J* = 9.0 Hz, 1H), 7.12 (t, *J* = 8.1 Hz, 1H), 6.96 (s, 1H), 6.39 (t, *J* = 8.7 Hz, 1H), 5.85 (dd, *J* = 9.3, 2.6 Hz, 1H), 5.72 (d, *J* = 7.1 Hz, 1H), 5.25 (s, 1H), 4.98 (d, *J* = 9.1 Hz, 1H), 4.80 (s, 1H), 4.36 (d, *J* = 8.3 Hz, 2H), 4.32–4.23 (m, 3H), 3.95 (d, *J* = 7.1 Hz, 1H), 2.67–2.55 (m, 1H), 2.46 (s, 3H), 2.41–2.24 (m, 4H), 1.90 (s, 4H), 1.79 (s, 3H), 1.22 (s, 3H), 1.13 (s, 3H). ¹³C NMR (125 MHz, CDCl₃) δ 211.17, 172.11, 170.64, 166.74, 163.38, 162.35, 161.85, 155.22, 137.98, 137.07, 136.26, 133.70, 130.76, 130.37, 129.44, 129.08, 128.78, 128.59, 127.10, 122.44, 117.74, 113.92, 106.03, 84.22, 81.27, 78.81, 74.81, 74.45, 73.42, 72.21, 71.90, 57.67, 54.79, 46.41, 43.12, 36.87, 36.03, 26.53, 22.63, 20.82, 14.42, 9.98. HRMS (FAB): calcd for C₄₈H₄₉N₂O₁₄F (M + NH₄⁺): 914.3506, found: 914.3490.

C3'-N-[3-(3-nitrophenyl) isoxazole-5-acyl]docetaxel (A3)

Yield: 70.8%. m.p. 195.2–196.7 °C. ¹H NMR (500 MHz, CDCl₃) δ 8.38 (s, 1H), 8.27 (d, *J* = 8.2 Hz, 1H), 8.22 (d, *J* = 7.3 Hz, 2H), 8.03 (d, *J* = 7.8 Hz, 1H), 7.86 (d, *J* = 9.3 Hz, 1H), 7.69 (t, *J* = 7.4 Hz, 1H), 7.59 (t, *J* = 7.8 Hz, 3H), 7.51 (d, *J* = 7.4 Hz, 2H), 7.46 (t, *J* = 7.5 Hz, 2H), 7.40 (d, *J* = 7.3 Hz, 1H), 7.11 (s, 1H), 6.35 (t, *J* = 8.6 Hz, 1H), 5.84 (dd, *J* = 9.3, 2.5 Hz, 1H), 5.70 (d, *J* = 7.1 Hz, 1H), 5.26 (s, 1H),

4.97 (d, *J* = 9.5 Hz, 1H), 4.82 (d, *J* = 2.4 Hz, 1H), 4.39–4.33 (m, 1H), 4.32–4.20 (m, 3H), 3.94 (d, *J* = 7.0 Hz, 1H), 2.65–2.54 (m, 1H), 2.45 (s, 3H), 2.38–2.25 (m, 4H), 1.94–1.84 (m, 5H), 1.78 (s, 3H), 1.21 (s, 3H), 1.13 (s, 3H). ¹³C NMR (125 MHz, CDCl₃) δ 211.17, 172.06, 170.61, 166.82, 163.99, 161.48, 155.01, 148.54, 137.98, 137.06, 136.26, 133.83, 132.34, 130.33, 129.33, 129.24, 129.10, 128.83, 128.63, 127.10, 125.17, 121.75, 105.78, 84.20, 81.26, 78.88, 74.82, 74.47, 73.34, 72.25, 71.93, 57.69, 54.80, 46.46, 43.08, 36.88, 35.92, 26.55, 22.64, 20.73, 14.44, 9.97. HRMS (FAB): calcd for C₄₈H₄₉N₃O₁₆ (M + NH₄⁺): 941.3451, found: 941.3437.

C3'-N-[3-(4-methoxyphenyl) isoxazole-5-acyl]docetaxel (A4)

Yield: 78.6%. m.p. 191.8–193.4 °C. ¹H NMR (500 MHz, CDCl₃) δ 8.26 (d, *J* = 7.5 Hz, 2H), 7.77 (d, *J* = 9.1 Hz, 1H), 7.67 (t, *J* = 7.4 Hz, 1H), 7.58 (t, *J* = 7.6 Hz, 2H), 7.52–7.44 (m, 5H), 7.41 (d, *J* = 7.1 Hz, 3H), 6.89 (s, 1H), 6.78 (d, *J* = 7.8 Hz, 2H), 6.45 (s, 1H), 5.88 (d, *J* = 7.4 Hz, 1H), 5.74 (d, *J* = 7.2 Hz, 1H), 5.26 (s, 1H), 4.99 (d, *J* = 9.2 Hz, 1H), 4.82 (s, 1H), 4.38–4.27 (m, 4H), 4.15 (br, s, 1H), 3.97 (d, *J* = 7.1 Hz, 1H), 3.85 (s, 3H), 2.66–2.58 (m, 1H), 2.49 (s, 3H), 2.43–2.33 (m, 3H), 1.96–1.88 (m, 5H), 1.81 (s, 3H), 1.24 (s, 3H), 1.14 (s, 3H). ¹³C NMR (125 MHz, CDCl₃) δ 211.32, 172.21, 170.56, 166.72, 162.91, 162.74, 161.38, 155.38, 137.95, 137.10, 136.31, 133.65, 130.41, 129.09, 128.76, 128.55, 128.16, 127.03, 114.35, 105.90, 84.18, 81.23, 78.81, 74.81, 74.48, 73.53, 72.24, 71.92, 57.65, 55.35, 54.65, 46.35, 43.16, 36.96, 36.10, 29.71, 26.52, 22.67, 20.90, 14.46, 10.02. HRMS (FAB): calcd for C₄₉H₅₂N₂O₁₅ (M + NH₄⁺): 926.3706, found: 926.3693.

C3'-N-[3-(4-chlorophenyl) isoxazole-5-acyl]docetaxel (A5)

Yield: 76.7%. m.p. 190.7–192.3 °C. ¹H NMR (500 MHz, CDCl₃) δ 8.27 (d, *J* = 7.3 Hz, 2H), 7.92 (d, *J* = 9.4 Hz, 1H), 7.67 (t, *J* = 7.4 Hz, 1H), 7.59 (t, *J* = 7.6 Hz, 2H), 7.50–7.38 (m, 6H), 7.32 (s, 1H), 7.21 (d, *J* = 8.2 Hz, 2H), 6.85 (s, 1H), 6.47 (t, *J* = 8.5 Hz, 1H), 5.87 (dd, *J* = 9.5, 2.6 Hz, 1H), 5.73 (d, *J* = 7.1 Hz, 1H), 5.25 (s, 1H), 4.99 (d, *J* = 9.5 Hz, 1H), 4.78 (s, 1H), 4.59–4.25 (m, 5H), 3.96 (d, *J* = 7.1 Hz, 1H), 2.66–2.59 (m, 1H), 2.50 (s, 3H), 2.44–2.27 (m, 3H), 1.96–1.88 (m, 5H), 1.80 (s, 3H), 1.22 (s, 3H), 1.12 (s, 3H). ¹³C NMR (125 MHz, CDCl₃) δ 211.19, 172.17, 170.63, 166.61, 163.33, 162.25, 155.17, 137.95, 137.00, 136.85, 136.28, 133.66, 130.45, 129.61, 129.25, 129.08, 128.80, 128.58, 127.84, 127.07, 125.48, 105.98, 84.23, 81.25, 78.85, 74.83, 74.40, 73.50, 72.11, 71.87, 57.64, 54.78, 46.33, 43.18, 36.86, 36.16, 26.49, 22.68, 21.00, 14.41, 10.04. HRMS (FAB): calcd for C₄₈H₄₉N₂O₁₄Cl (M + NH₄⁺): 930.3211, found: 930.3207.

The synthesis of C3'-N-amino-docetaxel (7)

To a stirred solution of **6** (1.35 g, 1 mmol) in AcOEt (20 mL) was added zinc powder (1.76 g, 27 mmol) and AcOH (3.5 mL) at room temperature. After 4 h, zinc powder was filtered off, water (20 mL) and NaHCO₃ (5.2 g) were added to the solution. The organic phase was washed with water and brine, dried over MgSO₄ and concentrated to get a crude compound, which was purified by column chromatography (CH₂Cl₂:MeOH = 7:1) to furnish a pure product **7** of 0.65 g as a white powder. Yield: 91.2%. m.p. 166.2–167.6 °C. ¹H NMR (400 MHz, DMSO) δ 7.95 (d, *J* = 7.1 Hz, 2H), 7.73 (t, *J* = 7.4 Hz, 1H), 7.65 (t, *J* = 7.5 Hz, 2H), 7.42 (d, *J* = 4.3 Hz, 4H), 7.28–7.19 (m, 1H), 5.85 (t, *J* = 8.7 Hz, 1H), 5.40 (d, *J* = 7.2 Hz, 1H), 5.09 (s, 1H), 5.04 (d, *J* = 7.1 Hz, 1H), 4.97 (s, 1H), 4.89 (d, *J* = 10.0 Hz, 1H), 4.53 (s, 1H), 4.22 (d, *J* = 7.9 Hz, 1H), 4.16 (d, *J* = 7.9 Hz, 1H), 4.10–3.96 (m, 3H), 3.63 (d, *J* = 7.2 Hz, 1H), 2.33–2.20 (m, 1H), 2.11 (s, 3H), 1.74 (s, 3H), 1.69–1.62 (m, 1H), 1.51 (s, 3H), 1.01 (s, 3H), 0.97 (s, 3H). ¹³C NMR (100 MHz, DMSO) δ 214.55, 177.74, 174.90, 170.41, 141.99, 141.07, 138.65, 135.24, 134.72, 133.89, 133.53, 133.09, 132.81, 88.93, 85.48, 82.06, 80.63, 80.37, 79.95, 78.97, 75.98, 75.04, 63.33, 62.18, 51.14, 48.09, 41.66, 40.19, 31.73, 27.64, 26.02, 18.94, 15.01. HRMS (FAB): calcd for C₃₈H₄₅NO₁₂ (M + H⁺) 708.3015, found: 708.3005.

Cytotoxicity assay

Cytotoxic activities were evaluated by using standard MTT assay after exposure of cells to the tested compounds for 72 h. Each experiment was performed at least three times. There was a good reproducibility between replicate wells with standard errors below 10%. The in vitro cytotoxicity of the synthesized compounds against different cancer cell lines was performed with the MTT assay according to the Mosmann's method. The MTT assay is based on the reduction of the soluble 3-(4,5-dimethyl-2-thiazolyl)-2,5-diphenyl-2*H*-tetrazolium bromide (MTT) into a bluepurple formazan product, mainly by mitochondrial reductase activity inside living cells. The cells used in cytotoxicity assay were cultured in improved RPMI 1640 medium supplemented with 10% fetal calf serum. Cells suspended in the medium were plated in 96-well culture plates and incubated at 37 °C in a 5% CO₂ incubator. After 24 h, the test sample was added to the cells in 96-well plates and cultured at 37 °C for 3 days. The cultured cells were mixed with 50 μL 5 mg/mL of MTT solution and incubated for 2 h at 37 °C. The supernatant was carefully removed from each well and 200 μL of DMSO was added to each well to dissolve the formazan crystals which were formed by the cellular reduction of MTT. After mixing with a mechanical

plate mixer, the absorbance of each well was measured by a microplate reader using a test wavelength of 570 nm. The results were expressed as the IC₅₀, which is the concentration of the drugs inducing a 50% inhibition of cell growth of treated cells when compared to the growth of control cells. Each experiment was performed at least three times. There was a good reproducibility between replicate wells with standard errors below 10%.

Immunocytochemistry assay the cell structures

Cells were fixed in suspension with 2% paraformaldehyde in phosphate buffered saline (PBS) on ice for 10 min. The cells were washed once with wash buffer (PBS containing 0.1% sodium azide), and resuspended in blocking buffer (PBS containing 5% serum), immobilized on round 12 mm coverslips by cytocentrifugation, and post-fixed with methanol at –20 °C for 10 min. The slides were washed twice with wash buffer and then blocked with blocking buffer, with shaking at room temperature for 30 min. The cells were stained with Actin-Tracker Green and Tubulin-Tracker-Red (Shanghai Yope Biotechnology, Shanghai, China). The cells were counterstained with Hoechst nuclear stain (Beyotime, 1:100).

Molecular docking simulations

In order to obtain the accurate binding poses of tubulin with the compounds **A1–A5**, all the docking simulations were investigated by the program GOLD 5.3 (Jones et al. 1995, 1997). The 3D structure of the compounds **A1–A5** were sketched using Maestro version (Schrodinger Inc.) and 2000 steps of optimization were performed in Amber12 with the GAFF force field (Wang et al. 2004; Case et al. 2012). Based on the high crystallographic resolution and R-factor, the crystal structure of tubulin from *Sus scrofa* (PDB ID: 2HXF, Chain A) was finally selected as the receptor for docking simulations. The receptor tubulin was performed 5000 steps minimization in Amber12 with the ff99SB force field (Case et al. 2012; Hummer et al. 2001). To obtain the best set of the docking parameters and the reliability of the docking results, the paclitaxel derived from the crystal structure of the complex tubulin was first docked into the binding site. The CO₂ atom coordinate of the paclitaxel was defined as the centroid of the binding site with 10 Å radius sphere. Recent studies demonstrated that ChemPLP was superior to the other scoring functions in GOLD for pose prediction (Chen et al. 2014; Yang et al. 2014; Tian et al. 2016a, b). ChemPLP score was employed to obtain the most accurate binding modes for **A1–A5**. The 2D interaction diagram was presented by the program Maestro version 10.1. Visualization of the structures was performed by PyMol1.3r1 edu (DeLano 2002).

Binding energy calculations

To compare the binding affinity of the analogs **A1–A5** with the receptor tubulin, the top docking pose for each analog that corresponded to the ChemPLP score was recorded by the Chemscore (Eldridge et al. 1997; Baxter et al. 1998). The Chemscore function was applied to measure affinity data by ranking the Chemscore delta value (Chen et al. 2014; Liu et al. 2014, 2015, 2016). Chemscore estimates the binding free energy ΔG according to Eq. (1):

$$\Delta G_{\text{binding}} = \Delta G_{\text{O}} + \Delta G_{\text{hbond}} + \Delta G_{\text{lipo}} + \Delta G_{\text{rot}} \quad (1)$$

The Chemscore function in our work can be written in the form:

$$\Delta G = -5.4800 + -3.3400 * S(\text{hbond}) + -0.1170 * S(\text{lipo}) + 2.5600 * H(\text{rot}) \quad (2)$$

Each component of this equation is the product of a term depending on the magnitude of a particular physical contribution to free energy (e.g., hydrogen bonding). The hydrogen bond term ($S(\text{hbond})$) is calculated for all complementary possibilities of hydrogen bonds between ligand atoms and receptor atoms. The lipophilic term ($S(\text{lipo})$) is calculated for all lipophilic ligand atoms and all lipophilic receptor atoms. $H(\text{rot})$ is used to estimate the flexibility penalty for molecules possessing frozen rotatable bonds (Eldridge et al. 1997).

Acknowledgements We gratefully acknowledge financial support of this work by the National Natural Science Foundation of China (21172262), the Chinese National Science & Technology Major Project (grants 2010ZXJ0900X-007), the Foundation of the 309th hospital (2015MS-011), the National Natural Science Foundation of China (grant number 21503272) and the General Financial Grant from the China Postdoctoral Science Foundation (grant number 2015M572753).

Compliance with ethical standards

Conflict of interest The authors declare that they have no conflict of interest.

References

- Baruchello R, Simoni D, Grisolia G, Barbato G, Marchetti P, Rondanin R, Mangiola S, Giannini G, Brunetti T, Alloati D et al. (2011) Novel 3,4-isoxazolidiamides as potent inhibitors of chaperone heat shock protein 90. *J Med Chem* 54:8592–8604
- Baxter CA, Murray CW, Clark DE, Westhead DR, Eldridge MD (1998) Flexible docking using tabu search and an empirical estimate of binding affinity. *Protein: Struct, Funct, Bioinforma* 33:367–382
- Case TADDA, Cheatham ITE, Simmerling JWCL (2012) AMBER12. University of California, San Francisco
- Chang J, Hao XD, Hao YP, Lu HF, Yu JM, Sun X (2013) Design, synthesis and cytotoxicity of novel 3'-n-alkoxycarbonyl docetaxel analogs. *Bioorg Med Chem Lett* 23:6834–6837
- Chen X, Liu J, Zhang Y (2014) Cantharidin impedes the activity of protein serine/threonine phosphatase in *plutella xylostella*. *Mol Biosyst* 10:240–250
- DeLano WL (2002) PyMOL molecular graphics system, version 1.3.0.4. LLC, Schrödinger
- Didier E, Fouque E, Commerçon A (1994) Expedient semisynthesis of docetaxel using 2-trichloromethyl-1,3-oxazolidine as side-chain protection. *Tetrahedron Lett* 35:3063–3064
- Eldridge MD, Murray CW, Auton TR, Paolini GV, Mee RP (1997) Empirical scoring functions: I. The development of a fast empirical scoring function to estimate the binding affinity of ligands in receptor complexes. *J Comput Aided Mol Des* 11:425–445
- Fu Y, Li S, Zu Y, Yang G, Yang Z, Luo M, Jiang S, Wink M, Efferth T (2009) Medicinal chemistry of paclitaxel and its analogues. *Curr Med Chem* 16:3966–3985
- Georg GI, Cheruvallath ZS, Himes RH, Mejillano MR, Burke CT (1992a) Synthesis of biologically active taxol analogues with modified phenylisoserine side chains. *J Med Chem* 35:4230–4237
- Georg GI, Cheruvallath ZS, Himes RH, Mejillano MR (1992b) Novel biologically active taxol analogues: Baccatin iii 13-(n-(p-chlorobenzoyl)-(2'r,3's)-3'-phenylisoserinate) and baccatin iii 13-(n-benzoyl-(2'r,3's)-3'-(p-chlorophenyl)isoserinate). *Bioorg Med Chem Lett* 2:295–298
- Georg GI, Boge TC, Cheruvallath ZS, Harriman GCB, Hepperle M, Park H, Himes RH (1994) Cheminform abstract: Schottenbaum acylation of n-debenzoyltaxol; an efficient route to n-acyl taxol analogues and their biological evaluation. *ChemInform* 25:no-no
- Gunda IG, Zacharia SC, Himes RH, Mejillano MR (1992) Semisynthesis and biological activity of taxol analogues: Baccatin iii 13-(n-benzoyl-(2'r,3's)-3'-(p-tolyl)isoserinate), baccatin iii 13-(n-(p-toluoyl)-2'r,3's)-3'-phenylisoserinate), baccatin iii 13-(n-benzoyl-(2'r,3's)-3'-(p-trifluoromethylphenyl)isoserinate), and baccatin iii 13-(n-(p-trifluoromethylbenzoyl)-(2'r,3's)-3'-phenylisoserinate). *Bioorg Med Chem Lett* 2:1751–1754
- Hayashi Y, Skwarczynski M, Hamada Y, Sohma Y, Kimura T, Kiso Y (2003) A novel approach of water-soluble paclitaxel prodrug with no auxiliary and no byproduct: design and synthesis of isotaxel. *J Med Chem* 46:3782–3784
- Hummer G, Rasaiah JC, Noworyta JP (2001) Water conduction through the hydrophobic channel of a carbon nanotube. *Nature* 414:188–190
- Ji Z, Ahmed AA, Albert DH, Bouska JJ, Bousquet PF, Cunha GA, Diaz G, Glaser KB, Guo J, Harris CM et al. (2008) 3-amino-benzo[d]isoxazoles as novel multitargeted inhibitors of receptor tyrosine kinases. *J Med Chem* 51:1231–1241
- Jones G, Willett P, Glen RC, Leach AR, Taylor R (1997) Development and validation of a genetic algorithm for flexible docking. *J Mol Biol* 267:727–748
- Jones G, Willett P, Glen RC (1995) Molecular recognition of receptor sites using a genetic algorithm with a description of desolvation. *J Mol Biol* 245:43–53
- Kingston DG, Snyder JP (2014) The quest for a simple bioactive analog of paclitaxel as a potential anticancer agent. *Acc Chem Res* 47:2682–2691
- Kirikae T, Ojima I, Kirikae F, Ma Z, Kuduk SD, Slater JC, Takeuchi CS, Bounaud PY, Nakano M (1996) Structural requirements of taxoids for nitric oxide and tumor necrosis factor production by murine macrophages. *Biochem Biophys Res Commun* 227:227–235

- Kirikae T, Ojima I, Ma Z, Kirikae F, Hirai Y, Nakano M (1998) Structural significance of the benzoyl group at the c-3'-n position of paclitaxel for nitric oxide and tumor necrosis factor production by murine macrophages. *Biochem Biophys Res Commun* 245:698–704
- Lamberth C, Kempf HJ, Kriz M (2007) Synthesis and fungicidal activity of n-2-(3-methoxy-4-propargyloxy) phenethyl amides. Part 3: stretched and heterocyclic mandelamide oomyceticides. *Pest Manage Sci* 63:57–62
- Lilienkamp A, Mao J, Wan B, Wang Y, Franzblau SG, Kozikowski AP (2009) Structure-activity relationships for a series of quinoline-based compounds active against replicating and non-replicating mycobacterium tuberculosis. *J Med Chem* 52:2109–2118
- Liu JY, Chen XE, Zhang YL (2015) Insights into the key interactions between human protein phosphatase 5 and cantharidin using molecular dynamics and site-directed mutagenesis bioassays. *Sci Rep* 5:12359
- Liu J, Tian Z, Zhang Y (2016) Structure-based discovery of potentially active semiochemicals for *Cydia pomonella* (L.). *Sci Rep* 6:34600
- Liu J, Yang X, Zhang Y (2014) Characterization of a lambda-cyhalothrin metabolizing glutathione s-transferase *cpgstd1* from *Cydia pomonella* (L.). *Appl Microbiol Biotechnol* 98:8947–8962
- Lu HF, Xie C, Chang J, Lin GQ, Sun X (2011) Synthesis, cytotoxicity, metabolic stability and pharmacokinetic evaluation of fluorinated docetaxel analogs. *Eur J Med Chem* 46:1743–1748
- Mekhail TM, Markman M (2002) Paclitaxel in cancer therapy. *Expert Opin Pharmacother* 3:755–766
- Mosmann T (1983) Rapid colorimetric assay for cellular growth and survival: application to proliferation and cytotoxicity assays. *J Immunol Methods* 65:55–63
- Ojima I, Fumero-Oderda CL, Kuduk SD, Ma Z, Kirikae F, Kirikae T (2003) Structure-activity relationship study of taxoids for their ability to activate murine macrophages as well as inhibit the growth of macrophage-like cells. *Bioorg Med Chem* 11:2867–2888
- Roh EJ, Kim D, Lee CO, Choi SU, Song CE (2002) Structure-activity relationship study at the 3'-n-position of paclitaxel: Synthesis and biological evaluation of 3'-n-acyl-paclitaxel analogues. *Bioorg Med Chem* 10:3145–3151
- Roh EJ, Song CE, Kim D, Pae HO, Chung HT, Lee KS, Chai KB, Lee CO, Un CS (1999) Synthesis and biology of 3'-n-acyl-n-debenzoylpaclitaxel analogues. *Bioorg Med Chem* 7:2115–2119
- Rowbottom MW, Faraoni R, Chao Q, Campbell BT, Lai AG, Setti E, Ezawa M, Sprankle KG, Abraham S, Tran L et al. (2012) Identification of 1-(3-(6,7-dimethoxyquinazolin-4-yloxy)phenyl)-3-(5-(1,1,1-trifluoro-2-methylpropyl)isoxazol-3-yl)urea hydrochloride (cep-32496), a highly potent and orally efficacious inhibitor of v-raf murine sarcoma viral oncogene homologue b1 (braf) v600e. *J Med Chem* 55:1082–1105
- Rowinsky EK (1997) The development and clinical utility of the taxane class of antimicrotubule chemotherapy agents. *Annu Rev Med* 48:353–374
- Shang YJ, Wang YG (2002) Synthesis of isoxazolines and isoxazoles using poly (ethylene glycol) as Suppor. *Synthesis* 12:1663–1668
- Swindell CS, Krauss N (2001) Syntheses of taxol, taxol analogs and their intermediates with variable A-ring side chain structures and compositions thereof. US Patent 6262281B1
- Tian Z, Liu J, Zhang Y (2016a) Key residues involved in the interaction between *Cydia pomonella* pheromone binding protein 1 (*cpmpbp1*) and codlemone. *J Agric Food Chem* 64:7994–8001
- Tian Z, Liu J, Zhang Y (2016b) Structural insights into *Cydia pomonella* pheromone binding protein 2 mediated prediction of potentially active semiochemicals. *Sci Rep* 6:22336
- Wang J, Wolf RM, Caldwell JW, Kollman PA, Case DA (2004) Development and testing of a general amber force field. *J Comput Chem* 25:1157–1174
- Yang XQ, Liu JY, Li XC, Chen MH, Zhang YL (2014) Key amino acid associated with acephate detoxification by *Cydia pomonella* carboxylesterase based on molecular dynamics with alanine scanning and site-directed mutagenesis. *J Chem Inf Model* 54:1356–1370